ELSEVIER

Journal of Alloys and Compounds 408–412 (2006) 989–994

Journal of ALLOYS AND COMPOUNDS

www.elsevier.com/locate/jallcom

Spectroscopic study of trivalent rare earth ions in calcium nitrate hydrate melt

Toshiyuki Fujii[a,*], Hideki Asano[b], Takaumi Kimura[c], Takeshi Yamamoto[d],
Akihiro Uehara[a], Hajimu Yamana[a]

[a] *Research Reactor Institute, Kyoto University, 2-1010 Asashiro Nishi, Kumatori, Sennan, Osaka 590-0494, Japan*
[b] *Department of Energy and Hydrocarbon Chemistry, Graduate School of Engineering, Kyoto University, Yoshida-Honmachi, Sakyo-ku, Kyoto 606-8501, Japan*
[c] *Department of Materials Science, Japan Atomic Energy Research Institute, Tokai, Ibaraki 319-1195, Japan*
[d] *Department of Nuclear Engineering, Graduate School of Engineering, Osaka University, 2-1 Yamadaoka, Suita, Osaka 565-0871, Japan*

Received 30 July 2004; received in revised form 6 December 2004; accepted 6 December 2004
Available online 13 June 2005

Abstract

Influence of the water content to chemical status of trivalent rare earth ions in calcium nitrate hydrate melt was studied by spectroscopic techniques. Fluorescence spectrometry for Eu(III) in $Ca(NO_3)_2{\cdot}RH_2O$ and electronic absorption spectrometry for Nd(III) in $Ca(NO_3)_2{\cdot}RH_2O$ were performed for analyzing the changing coordination symmetries through the changes in their hypersensitive transitions. Raman spectroscopic study and EXAFS study were performed for $Y(NO_3)_3$ solutions and Y(III) in $Ca(NO_3)_2{\cdot}RH_2O$ for analyzing the oxygen bonding to Y(III). Luminescence lifetime study of Eu(III) and Dy(III) in $Ca(NO_3)_2{\cdot}RH_2O$ was performed for evaluating the hydration number changes. Results of these spectroscopic studies indicated that, with the decrease of water content (R), the hydration number decreases while the interaction between trivalent rare earth ion and nitrate ion increases. It was also revealed that the symmetry of the coordination sphere gets distorted gradually by this interaction.
© 2005 Elsevier B.V. All rights reserved.

Keywords: Fluorescence spectroscopy; Luminescence lifetime; EXAFS; Calcium nitrate; Hydrate melt

1. Introduction

Calcium nitrate hydrate melt, $Ca(NO_3)_2{\cdot}RH_2O$ with R less than about 6, can be recognized as an extremely highly concentrated electrolyte media with limited amount of water, and it gives quite characteristic chemical behavior to the solute in it. Characteristics variation of the activity coefficients of trivalent lanthanides dissolved in $Ca(NO_3)_2{\cdot}RH_2O$ with R less than 5.7 has been reported by the study on extraction equilibria of trivalent f-elements between TBP in *n*-dodecane and $Ca(NO_3)_2{\cdot}RH_2O$ [1–3].

For investigating the mechanism of the characteristic variation of the activity coefficient of lanthanides in hydrate melts, spectroscopic techniques are effective, because we can observe directly the change of the chemical circumstances of cations in the hydrate melt. In our previous study [4], in which ν_4 vibration of nitrate ion $NO_3{}^-$ in $Ca(NO_3)_2{\cdot}RH_2O$ was studied by Raman spectrometry, it was suggested that the hydrated waters in the coordination sphere of Ca^{2+} are probably displaced by nitrate ions. We can expect a similar effect to the cations (trivalent rare earth ions) dissolved in $Ca(NO_3)_2{\cdot}RH_2O$.

In the present study, some spectroscopic techniques were applied to study the interaction between trivalent rare earth ions and nitrate ions in the calcium nitrate hydrate melt. Fluorescence spectrometry, absorption spectrometry, Raman

---

[*] Corresponding author. Tel.: +81 724 51 2469; fax: +81 724 51 2634.
E-mail address: tosiyuki@hl.rri.kyoto-u.ac.jp (T. Fujii).

0925-8388/$ – see front matter © 2005 Elsevier B.V. All rights reserved.
doi:10.1016/j.jallcom.2004.12.117

spectrometry, EXAFS analysis, and luminescence lifetime analysis were performed.

2. Experimental

2.1. Fluorescence spectrometry

Calcium nitrate tetrahydrate of analytical grade (Wako Chemical Industries Ltd.) was used without further purification. $Ca(NO_3)_2 \cdot RH_2O$ having five different water content was prepared ($R = 4.0, 5.0, 6.0, 7.0$, or 8.0). Concentration of europium in those melts was [Ca]/[Eu] = 1000. Each melt was transferred into a quartz cell, sealed with a stopcock, and kept at 343 K in a water bath. Just after taking each of them out of the bath, the fluorescence spectrum was measured within 40 s at 394 nm excitation by a fluorescence spectrophotometer, HITACHI, F-2500. The temperature change of the samples during the measurement was less than ca. 5 K.

2.2. Luminescence lifetime analysis

0.01 mol dm^{-3} (M) Eu^{3+} or 0.01 M Dy^{3+} in $Ca(NO_3)_2 \cdot RH_2O$ having various water content was prepared. Dy^{3+} in $Ca(NO_3)_2 \cdot RH_2O$ was excited to the $^4I_{11/2}$ excited states at 355 nm by a 355 nm pulsed laser beam. Eu^{3+} in $Ca(NO_3)_2 \cdot RH_2O$ was excited to the $^5L_6$ excited states at 394 nm by a 390–410 nm laser beam. The emission light was collected at 90° into a monochromator and detected by a photomultiplier tube. The experiment was performed at 323 K. Detailed conditions of experimental apparatus can be seen elsewhere [5]. The obtained luminescence decay curves were fitted to single-exponential curves.

2.3. Absorption spectrometry

$Ca(NO_3)_2 \cdot RH_2O$ ($R = 4.0, 5.0, 6.0, 7.0$, or 8.0) containing neodymium as [Ca]/[Nd] = 1000 were prepared. Each melt was transferred into a quartz cell, which was sealed with a stopcock, and kept at 343 K in a water bath. Just after taking each of them out of the bath, the absorption spectrum from 555 to 597 nm was measured by an absorption spectrophotometer (ACTON Research Co.) within 15 s.

2.4. Raman spectrometry

$Y(NO_3)_3 \cdot 6H_2O$ was obtained from Kojundo Chemical Laboratory Co. Ltd., 2 M $Y(NO_3)_3$ solution, and saturated $Y(NO_3)_3$ solution (at room temperature) were prepared. Raman spectra of these two solutions and $Y(NO_3)_3 \cdot 6H_2O$ (solid) were measured by an excitation using the 514.5 nm of Ar^+ laser (NEC, GLS 3280 and GLG 3280) and recorded by a JASCO NR-1100 spectrophotometer at 0.1 cm^{-1} intervals and 60 cm^{-1} per minute scanning rate. The laser power applied was 300 mW (liquid) or 100 mW (solid). The analysis was performed at room temperature.

2.5. EXAFS analysis

0.7 M solutions of $Y(NO_3)_3$ in $Ca(NO_3)_2 \cdot RH_2O$ ($R = 3.5$, 4.0, 8.0, or 51.6) were prepared. 0.2 M $Y(NO_3)_3$ solution and 2 M $Y(NO_3)_3$ solution without $Ca(NO_3)_2$ were also prepared. EXAFS measurement was performed using a laboratory-type instrument of TECHNOS Co. Ltd. (EXAC820). A transmission-mode measurement was adopted using a GeSSD detector. Spectra were taken at yttrium K-edge (17.041 keV) with a Ge(840) monochromator. Measurement was performed at room temperature, but the hydrate melt samples remained to be a super-cooled liquid during the measurement. Obtained XAFS raw data were treated by WinXAS ver. 2.0 [6].

The pre-edge absorption threshold was determined from the first derivative of the near-edge region. The pre-edge background, which can be fitted using Vicroreen function, was subtracted from EXAFS spectrum. Cubic splines were used to fit and to subtract the atom-like background. The k^3-weight XAFS spectra were Fourier-transformed assuming a Gaussian window function. In the R space, EXAFS data were reconstructed by using two or three paths calculated from the simulation of the model structures with FEFF8 [7] program.

3. Results and discussion

3.1. Fluorescence spectrometry

Eu(III) complexes in liquids essentially emanate emission lights from the nondegenerate $^5D_0$ level, when excitation is over the $^5D_0$ level. The strongest emissions are observed in the $^5D_0 \rightarrow {}^7F_1$ and $^5D_0 \rightarrow {}^7F_2$ transition regions. The $^5D_0 \rightarrow {}^7F_2$ transition is predominantly electric dipole in character, and its radiative transition probability is very sensitive (hypersensitive) to the nature of the ligand environment. In the low symmetry systems, its emission probability drastically increases. On the other hand, even in low symmetry systems, the $^5D_0 \rightarrow {}^7F_1$ transition retains its magnetic dipole character, and its radiative transition probability is not much affected by the ligand environment. Hence, the relative intensities of the $^5D_0 \rightarrow {}^7F_1$ and $^5D_0 \rightarrow {}^7F_2$ emissions are useful to know the nature of the ligand environment [8].

Fluorescence spectra of Eu(III) in $Ca(NO_3)_2 \cdot RH_2O$ are shown in Fig. 1, which is standardized to the peak intensity of $^5D_0 \rightarrow {}^7F_1$ transition. With the decrease of water content, the relative intensities of the $^5D_0 \rightarrow {}^7F_1$ to $^5D_0 \rightarrow {}^7F_2$ emissions increased, reflecting the hypersensitive character of the $^5D_0 \rightarrow {}^7F_2$ transition. This indicates that the distortion of the symmetry of Eu(III) complex in $Ca(NO_3)_2 \cdot RH_2O$ proceeds with decreasing water content. This is attributable to the change of the hydration status, possibly to the change of the hydration number, or to the promotion of the displacement of hydrated waters with nitrate ions generated.

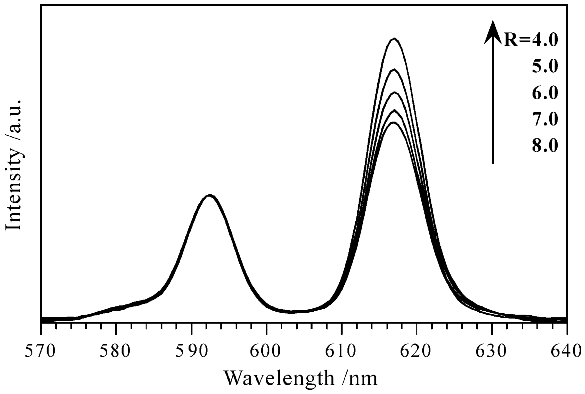

Fig. 1. Fluorescence spectra of Eu(III) in $Ca(NO_3)_2 \cdot RH_2O$. $[Ca^{2+}]/[Eu^{3+}] = 1000$, temperature = 343 K.

3.2. Emission lifetime analysis

In order to characterize the hydration of rare earth complex in $Ca(NO_3)_2 \cdot RH_2O$, we estimated hydration numbers (N_{H_2O}) of Eu(III) and Dy(III) in $Ca(NO_3)_2 \cdot RH_2O$. By the method already verified [8], the following relationships were used:

$$N_{H_2O} = 1.05 \times 10^{-3} k_{obs}(\text{Eu}) - 0.44 \quad (1)$$

$$N_{H_2O} = 2.11 \times 10^{-5} k_{obs}(\text{Dy}) - 0.60 \quad (2)$$

where k_{obs} is the luminescence decay constant. The obtained N_{H_2O} values are shown in Fig. 2 as functions of water activity, $\log a_{H_2O}$.

For aqueous systems, the light lanthanides form a series with the hydration number of 9, whereas the heavier ones form octahydrates. This can be seen in Fig. 2, in which N_{H_2O}'s of Eu(III) and Dy(III) give 8–9 in the water abundant region, and N_{H_2O} of Eu(III) is larger than that of Dy(III) throughout the experimental region of $\log a_{H_2O}$. It can be seen that, for both elements, the N_{H_2O} values decrease with the decrease of water content, and they lose as many as two in the hydrate melt region.

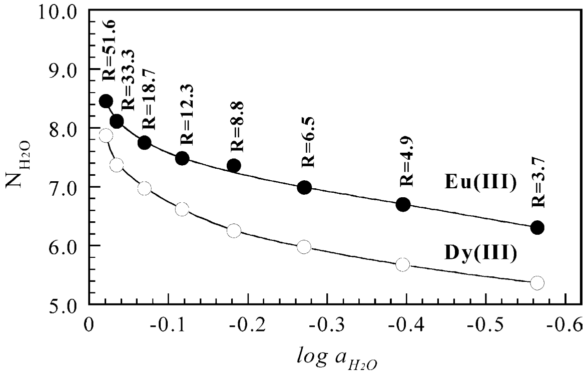

Fig. 2. Hydration numbers of Eu(III) and Dy(III) in $Ca(NO_3)_2 \cdot RH_2O$. $[Eu^{3+}]$, $[Dy^{3+}] = 0.01$ M, temperature = 323 K. Water activities were determined for $Ca(NO_3)_2 \cdot RH_2O$ at 343 K [3].

3.3. Absorption spectrometry

The electric dipole transition between f-orbitals that show abnormal variations in intensity are classified as hypersensitive transitions. These variations are attributed to the action of an inhomogeneous electromagnetic field from medium. In the case of neodymium, transitions from the ground level $^4I_{9/2}$ to excited levels of $^2G_{7/2}$ and $^4G_{5/2}$, which are abbreviated as $^4G_{5/2}, {}^2G_{7/2} \leftarrow {}^4I_{9/2}$, are sensitive with the coordination circumstances, and they are commonly used to examine the coordination of Nd^{3+} [9]. The transition $^4G_{5/2} \leftarrow {}^4I_{9/2}$ is known as the hypersensitive transition, which is accompanied and overlapped with a less intensive non-hypersensitive transition to the level $^2G_{7/2}$.

From the intensities of the measured absorption bands corresponding to the $^4G_{5/2}, {}^2G_{7/2} \leftarrow {}^4I_{9/2}$ transitions of Nd(III), the molar absorptivity of the $^4G_{5/2} \leftarrow {}^4I_{9/2}$ transition was found to increase in $Ca(NO_3)_2 \cdot RH_2O$ with the decrease of water content. The oscillator strength, which is an index for the transition probability being calculated from the molar absorptivity, was obtained for the $^4G_{5/2}, {}^2G_{7/2} \leftarrow {}^4I_{9/2}$ transitions in the 555–597 nm region. The oscillator strength is defined as

$$f = 4.319 \times 10^{-9} \{9n/(n^2+2)^2\} \int \varepsilon(\nu) d\nu \quad (3)$$

where $\varepsilon(\nu)$ is the molar absorptivity at energy ν (cm^{-1}) and n is the refractive index of the solvent medium. In the present study, n values of $Ca(NO_3)_2 \cdot RH_2O$ measured with a refractometer at room temperature were adopted to Eq. (3). The obtained f values are shown in Fig. 3 as a function of water activity, $\log a_{H_2O}$. The shift of peak position of the $^4G_{5/2} \leftarrow {}^4I_{9/2}$ transition was also shown in Fig. 3.

At a fixed temperature, the factors influencing f value of Nd(III) hypersensitive transition in $Ca(NO_3)_2 \cdot RH_2O$ are: (i) symmetry of Nd(III) complex and (ii) electron donating ability of oxygenatom involved in attached H_2O and NO_3^-. The observed increase of the f value with the decrease of water content suggests the increasing distortion of symmetry of Nd(III) complex. Both the decrease of the hydration number and/or direct coordination of nitrate ion are considered

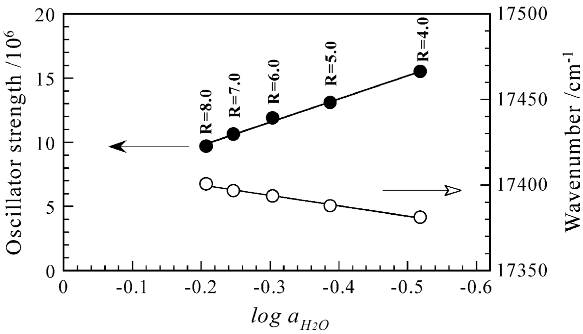

Fig. 3. Oscillator strength and peak position of the hypersensitive transitions of Nd(III) in $Ca(NO_3)_2 \cdot RH_2O$. $[Ca^{2+}]/[Nd^{3+}] = 1000$, temperature = 343 K. Water activities were determined for $Ca(NO_3)_2 \cdot RH_2O$ at 343 K [3].

to promote this distortion. The increase of *f* also suggests the increase of electron donating ability of oxygen atom of water or nitrate. The possible increase of the electron donation from the ligands with the decreasing water content can be also confirmed by the observed shift of the peaks to the lower energy direction. It is known that an overlap of the electron clouds between the central atom and the ligands leads to a shift of absorption bands towards smaller energy, and this is known as the nephelausetic effect [10]. Since the electron donating ability (covalency) of oxygen in H_2O is weaker than that in NO_3^-, the substitution would result in the increase of the averaged covalency of oxygen atoms in the coordination sphere of Nd(III), and this agree with the observed peak shift of the $^4G_{5/2} \leftarrow {}^4I_{9/2}$ transition to the smaller energy with the decrease of water content (Fig. 3).

3.4. Raman spectrometry

The ν_4 vibration of NO_3^- can be seen in the 700–760 cm^{-1} region. In the previous study [7], we have reported the ν_4 vibrational spectra of NO_3^- in the various water content $Ca(NO_3)_2 \cdot RH_2O$ at 343 K. It was found [7] that the Raman peak at 720 cm^{-1} was observed at high water content, but it decreased with decreasing water content. On the contrary, a peak at 740 cm^{-1} grew along with the decrease of water content. It can be understood that the peak at 720 cm^{-1}, which corresponds to free nitrate [11], decreased along with lower *R*, as a result of the promoted direct coordination of nitrate to Ca^{2+}. This is consistent with the growth of 740 cm^{-1} peak, which corresponds to the nitrate ion directly coordinated to Ca^{2+} [4,11].

Fig. 4 shows the ν_4 vibrational spectra of NO_3^- in $Y(NO_3)_3 \cdot 6H_2O$, 2 M $Y(NO_3)_3$, and saturated $Y(NO_3)_3$ solution. Similar to the case of $Ca(NO_3)_2 \cdot RH_2O$, clear Raman peaks can be seen. With the decrease of water content, the Raman intensity of the lower frequency vibration decreased, whereas that of the higher one increased. This can be considered as the evidence of the increase of direct coordination of nitrate to yttrium in $Y(NO_3)_3 \cdot RH_2O$ with smaller *R*. Similar effect can be expected in dissolved yttrium in ions in $Ca(NO_3)_2 \cdot RH_2O$ having small *R*. The results of the previous study [4] and this study suggests that, for the trivalent rare earth, hydrated waters are displaced by nitrate ions with the decrease of water content.

3.5. EXAFS analysis

Fig. 5a shows k^3 weighted EXAFS spectra of Y(III) in $Ca(NO_3)_2 \cdot 4H_2O$, and its Fourier transforms are shown in Fig. 5b. In the present analysis, distances of Y–O (hydrated water) and Y–O (nitrate ion) cannot be separated, and thus the averaged Y–O distance can be determined.

Crystal ionic radius of Y^{3+} with coordination number 8 is similar to that of heavy lanthanide, cf. Ho^{3+}, and yttrium is expected to represent the characteristics of heavy lanthanides. An EXAFS study on Y^{3+} in $HClO_4$ solution has reported the coordination number 8.0–8.2 [12], but higher coordination numbers have been reported for $Y(NO_3)_3$ solution [13] and YBr_3 solution [14]. We performed the analysis on assumption of coordination number 8.0 and 9.0, and thus the smaller Deby–Waller factors were obtained for 8.0. The structural parameters of the $Y(NO_3)_3$ solutions and Y(III) in $Ca(NO_3)_2 \cdot RH_2O$, which were determined on the coordination number 8.0, are given in Table 1. For the water abundant systems, 0.2 M $Y(NO_3)_3$ solution and 0.7 M Y(III) in $Ca(NO_3)_2 \cdot 51.6H_2O$, the determined Y-O distances are 2.35 and 2.36, respectively. These values are close to the reported values, 2.35–2.37, for aqueous systems [12–14].

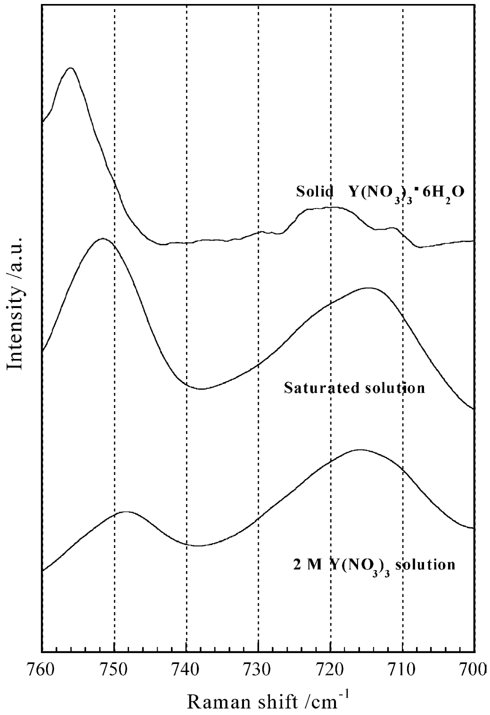

Fig. 4. Raman spectra of 2.0 M $Y(NO_3)_3$ solution, saturated $Y(NO_3)_3$ solution, and solid $Y(NO_3)_3 \cdot 6H_2O$.

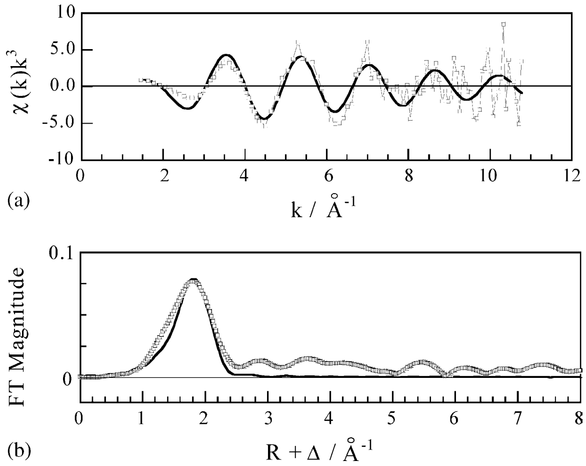

Fig. 5. k^3 weighted EXAFS spectra of Y(III) in $Ca(NO_3)_2 \cdot 4H_2O$ (a), and its Fourier transforms (b). $[Y^{3+}] = 0.7$ M.

Table 1
Structural parameters of $Y(NO_3)_3$ solutions and Y(III) in $Ca(NO_3)_2 \cdot RH_2O$

Sample	Coordination number, N	Interatomic distance, r(Y–O) (Å)	Deby–Waller factor, σ^2 (Å^2)	Energy shift, E_0 (eV)
0.2 M $Y(NO_3)_3$	8.0	2.35	0.0065	−7.1
2.0 M $Y(NO_3)_3$	8.0	2.40	0.0065	−7.1
0.7 M $Y(NO_3)_3$ in $Ca(NO_3)_2 \cdot 3.5H_2O$	8.0	2.39	0.0065	−7.1
0.7 M $Y(NO_3)_3$ in $Ca(NO_3)_2 \cdot 4.0H_2O$	8.0	2.42	0.0065	−7.1
0.7 M $Y(NO_3)_3$ in $Ca(NO_3)_2 \cdot 8.0H_2O$	8.0	2.38	0.0065	−5.4
0.7 M $Y(NO_3)_3$ in $Ca(NO_3)_2 \cdot 51.6H_2O$	8.0	2.36	0.0065	−7.1

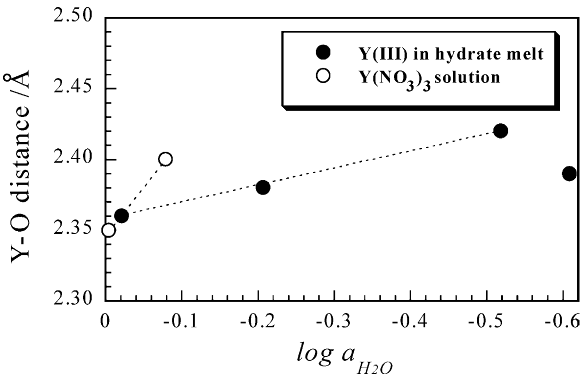

Fig. 6. Dependence of Y–O distance on water activity. For Y(III) in $Ca(NO_3)_2 \cdot RH_2O$, water activities of $Ca(NO_3)_2 \cdot RH_2O$ at 343 K [3] were adopted. Since water activities of $Y(NO_3)_3$ solutions were not available, reported a_{H_2O} values of $La(NO_3)_3$ solutions at 298.2 K [15] were used.

The Y–O distances are shown in Fig. 6 as functions of $\log a_{H_2O}$. Both $Y(NO_3)_3$ solutions and Y(III) in $Ca(NO_3)_2 \cdot RH_2O$ showed increasing trend of Y–O distance with the decrease of water content. One exception of the increasing trend was found for the point of 0.7 M $Y(NO_3)_3$ in $Ca(NO_3)_2 \cdot 3.5H_2O$, but this is probably due to the freezing of the sample during the EXAFS measurement. By the crystal structure data of yttrium nitrate monohydrate [16] and yttrium nitrate trihydrate [17], it is known that the Y–O (nitrate ion) distance is longer than that of Y–O (hydrated water). Therefore, the observed increasing trend of Y–O distance in both $Y(NO_3)_3$ solutions and Y(III) in $Ca(NO_3)_2 \cdot RH_2O$ is considered to be the result of the nitrate coordination to yttrium, which was promoted under water deficient conditions. It is quite probable that the substitution of hydration waters by nitrate ions proceeds in hydrate melts, and this result of EXAFS is in accordance with the results by other methods

4. Conclusion

Five spectroscopic techniques were used to analyze the coordination status of lanthanides in $Ca(NO_3)_2 \cdot RH_2O$ hydrate melt. By fluorescence and absorption spectrometry, the increase of the distortion of the coordination symmetry of the rare earth complex and the electron donating ability, with the decrease of water content, were observed. Luminescence lifetime analysis clearly showed the decrease of hydration water around the lanthanide along with the decrease of water content. Raman spectroscopy showed an increase in the direct coordination of nitrate to the lanthanide with the decrease of water, and EXAFS confirmed it through the longer Y–O distance in water deficient systems. All these results support the simultaneous decrease of hydration and increase of nitrate coordination, that is to say, substitution of hydration water with nitrate ion, under the condition of decreasing water in $Ca(NO_3)_2 \cdot RH_2O$ hydrate melt. This gradual change of coordination status of lanthanides in hydrate melt explains the increase of their activity coefficient in water deficient hydrate melts, but it can not explain the peculiar trend of their activity coefficients in $Ca(NO_3)_2 \cdot RH_2O$ of lower R than 5.7.

Acknowledgments

The authors are grateful to Mr. Hiroaki Furukawa of TECHNOS Co. Ltd., for his technical supports on the EXAFS measurement. The authors wish to thank Mr. Roy Jacobus for his help in improving the English expressions of this paper.

References

[1] H. Yamana, T. Kaibuki, Y. Miyashita, S. Shibata, H. Moriyama, J. Alloys Compd. 271–273 (1998) 701.
[2] H. Yamana, T. Kaibuki, H. Moriyama, Radiochim. Acta 84 (1999) 191.
[3] H. Yamana, H. Asano, T. Fujii, R. Gohtoh, H. Moriyama, Radiochim. Acta 90 (2002) 87.
[4] T. Fujii, H. Yamana, H. Moriyama, J. Nucl. Sci. Technol. Suppl. 3 (2002) 336.
[5] T. Kimura, Y. Kato, J. Alloys Compd. 275–277 (1998) 806.
[6] T. Ressler, J. Phys. IV 7 (1997) C2.
[7] L. Ankudinov, B. Ravel, J.J. Rehr, S.D. Conradson, Phys. Rev. B 57 (1998) 7518.
[8] F.S. Richardson, Chem. Rev. 82 (1982) 541.
[9] K.B. Yatsimirskii, N.K. Davidenko, Coord. Chem. Rev. 27 (1979) 223.
[10] C.K. Jørgensen, Prog. Inorg. Chem. 4 (1962) 73.
[11] H. Kanno, J. Hiraishi, J. Phys. Chem. 88 (1984) 2787.
[12] P. Lindqvist-Reis, K. Lamble, S. Pattanaik, I. Persson, M. Sandström, J. Phys. Chem. B 104 (2000) 402.
[13] K. Vala Ragnarsdottir, E.H. Oelkers, D.M. Sherman, C.R. Collins, Chem. Geol. 151 (1998) 29.

[14] S. Díaz-Moreno, A. Muñoz-Páez, J. Chaboy, J. Phys. Chem. A 104 (2000) 1278.

[15] G.G. Aseyev, Electrolytes: Equilibria in Solutions and Phase Equilibria, Begell House, Inc. Publishers, New York, 1999.

[16] B. Ribár, P. Radivojević, G. Argay, A. Kálmán, Acta Cryst. C46 (1990) 525.

[17] B. Ribár, P. Radivojević, G. Argay, A. Kálmán, Acta Cryst. C44 (1988) 595.